Available online at www.sciencedirect.com
SCIENCE DIRECT®
Biochemical and Biophysical Research Communications 338 (2005) 262–266
BBRC
www.elsevier.com/locate/ybbrc

Reactions of the diiron(IV) intermediate Q in soluble methane monooxygenase with fluoromethanes

Laurance G. Beauvais, Stephen J. Lippard *

Department of Chemistry, Massachusetts Institute of Technology, Cambridge, MA 02139, USA

Received 15 July 2005
Available online 8 September 2005

Abstract

Soluble methane monooxygenases utilize a carboxylate-bridged diiron center and dioxygen to convert methane to methanol. A diiron(IV) oxo intermediate Q is the active species for this process. Alternative substrates and theoretical studies can help elucidate the mechanism. Experimental results for reactions with derivatized methanes were previously modeled by a combination of quantum mechanical/molecular mechanical techniques and the model was extended to predict the relative reactivity of fluoromethane. We therefore studied reactions of Q with CF_nH_{4-n} ($n = 1$–3) to test the prediction. The kinetics of single-turnover reactions of Q with these substrates were monitored by double-mixing stopped-flow optical spectroscopy. For fluoro- and difluoromethane, conversion to the alcohols occurred with second-order rate constants less than that of methane, the values being 28,700 (CH_4) > 25,000 (CFH_3) > 9300 (CF_2H_2) $M^{-1}\,s^{-1}$. KIE values for C–H versus C–D activation above the classical limit were observed, requiring modification of the theoretical predictions.

Keywords: Soluble methane monooxygenase; Hydroxylase; Fluorocarbon oxidation; Dioxygen activation; Enzyme kinetics

Elucidating the mechanisms of catalysis of metalloenzymes benefits from information about the structures of reactive intermediates. The transient nature of these species usually prohibits their study by X-ray diffraction, and structural information must be gleaned from spectroscopic studies of freeze-quenched intermediates when available. Theoretical analyses of metalloenzyme catalytic cycles provide additional insight into transition state and intermediate geometries, as well as their energies [1–3], but corroborative experimental data are required to calibrate the computational models. Soluble methane monooxygenase (sMMO) has proved to be an enzymatic system well suited for this type of work, because its intermediates are amenable to stopped-flow and rapid-freeze quench spectroscopic analysis [4]. sMMO has therefore been the focus of much theoretical work [5–7]. Recently, quantum mechanical/molecular mechanical (QM/MM) calculations have afforded activation barriers and rate constants [8] that agree with stopped-flow studies of the reactions of substituted methanes with the diiron(IV) oxo intermediate (Q) in the catalytic cycle of sMMO [9]. In addition, the theoretical study predicted results for the reaction of Q with fluoromethane [8].

Studies using sMMO isolated from *Methylococcus capsulatus* (Bath) (*Mc*) and *Methylosinus trichosporium* OB3b (*Mt*) reveal that substrate hydroxylation occurs at a carboxylate-bridged diiron center residing in the α subunit of the hydroxylase protein MMOH, a 251-kDa $\alpha_2\beta_2\gamma_2$ heterodimer [4,10]. In addition, two other proteins are required for activity in vivo, a 38.5-kDa reductase MMOR, which receives electrons from NADH and then transfers them to MMOH, and a 16-kDa regulatory protein MMOB, which is necessary for efficient catalysis. Various spectroscopic techniques revealed the existence of intermediates in the reaction of reduced MMOH (H_{red}) with dioxygen in the presence of 2 equiv. of MMOB (Fig. 1). In the absence of substrate, the first observable intermediate

* Corresponding author. Fax: +1 617 253 8150.
E-mail address: lippard@mit.edu (S.J. Lippard).

0006-291X/$ - see front matter © 2005 Elsevier Inc. All rights reserved.
doi:10.1016/j.bbrc.2005.08.220

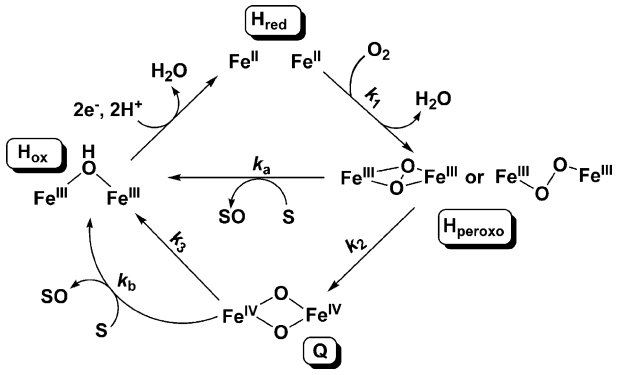

Fig. 1. Species observed in the catalytic cycle of soluble methane monooxygenase. Note that H_{peroxo} and Q are both capable of reacting with substrates.

H_{peroxo} rapidly converts to Q, which slowly decays to afford oxidized protein (H_{ox}) [4]. Although the independent reactivity of H_{peroxo} has only recently been demonstrated [11,12], extensive data have been reported for reactions of Q with a wide range of substrates [9,13].

Studies of MMOH reactions with substrates other than methane provide valuable information for understanding the hydroxylation mechanism. Reactions with radical clock substrate probes indicate that no discrete alkyl radical forms during the hydroxylation of hydrocarbon substrates [5]. Reactions of Q with methane analogs CH_3X, where $X = CH_3$, OH, CN, and NO_2, can be divided into two classes [14] depending upon whether C–H activation (Class I) or substrate binding (Class II) is rate-limiting [8,9,13,15]. Reactions of Q with methane and acetonitrile exhibit kinetic isotope effects (KIEs) larger than the classical limit, indicating that C–H activation occurs with tunneling at the transition state, whereas the KIE for nitromethane is typical for classical C–H bond activation. For ethane and methanol, the KIE = 1, which signals substrate binding as the rate-limiting step. These results have been analyzed by QM/MM techniques in which the QM model incorporated ~100 atoms and the MM model approximately 7200 atoms within 35 Å of the active site [8]. The theoretical study revealed that the barrier for substrate binding is larger than that for C–H bond activation for ethane and methanol, and there was a large barrier for C–H activation of nitromethane, which would give rise to a classical value for the KIE. In addition, the barrier for C–H activation of fluoromethane was calculated to be larger than for methane due to an unfavorable electrostatic interaction with the carbonyl oxygen atom of Gly113 in the enzyme active site and a large entropy loss upon substrate binding. Given the large barrier to reaction and the endothermicity for the formation of the $^{\bullet}CH_2F$ radical from CH_3F, which is nearly equal to that of $^{\bullet}CH_2NO_2$ from CH_3NO_2, it was predicted that the KIE for fluoromethane would approach the classical value of 8.1 observed for nitromethane.

To test this prediction and extend the range of fluorinated methanes, we investigated by transient spectroscopy the reactions of Q with CF_nH_{4-n} ($n = 1$–3) and their deuterated analogs. Kinetic data are presented in this report and discussed in terms of the QM/MM model.

Methods and materials

Materials. The hydroxylase protein was purified from *Mc* cells as previously described [12,16]. The regulatory and reductase proteins were expressed recombinantly in *Escherichia coli* and purified as reported elsewhere [17,18]. High activity enzyme was employed for these studies [12]. Distilled water was deionized with a Milli-Q filtering system. Other reagents were of commercial origin and used as received.

Stopped-flow optical spectroscopy. Transient kinetics experiments were performed with a Hi-Tech Scientific (Salisbury, UK) SF-61 DX2 stopped-flow thermostatted spectrophotometer described previously [11]. The hydroxylase enzyme was reduced with dithionite and methyl viologen in the presence of 2 equiv. of MMOB in 25 mM potassium phosphate (pH 7.0) solution. The concentration of H_{red}:2B in the optical cell was 25 μM. Intermediate Q was generated by rapidly mixing fully reduced hydroxylase (H_{red}) in anaerobic buffered solution containing 2 equiv. of MMOB with O_2-saturated buffer in the initial push of a double-mixing experiment. After a specified time delay that coincides with the maximal concentration of Q, substrate-containing buffered solution was introduced in a second push to initiate the hydroxylation reaction. Reaction time courses were monitored at 420 nm with a photomultiplier detector. Data collection and analysis were performed by using KinetAsyst 3 (Hi-Tech Scientific) and KaleidaGraph v. 3.51 (Synergy Software) software. The data were fit to rate constants for single-exponential decay.

Substrate solutions were prepared by exposing vacuum-degassed buffer solutions to substrate and stored in gas-tight bombs. Before each set of experiments, the substrate concentration was determined by ^{19}F NMR spectroscopy employing NaF as an internal standard, except for fluoroform. The saturation concentration of fluoroform at 25 °C was calculated from the published solubility data [19]. The substrate solutions were diluted to achieve the desired concentration by using gastight syringes fitted with three-way valves.

NMR spectroscopy. ^{19}F NMR spectra were recorded on a Varian Mercury 300 MHz spectrometer in 25 mM potassium phosphate (pH 7.0) solution and chemical shifts are reported versus $CFCl_3$. A solution of 29 mM NaF was used as an internal shift ($\delta = -133$, s) [20] and concentration standard. All spectra were recorded at 20 °C. The chemical shifts for the substrates were CH_3F ($\delta = 279$, q), CD_3F ($\delta = 280$, m), CH_2F_2 ($\delta = -156$, t), and CD_2F_2 ($\delta = -157$, m), in close agreement with previously reported values for the protio-substrates [21].

Results

The decay rate of intermediate Q is substantially accelerated in the presence of fluoromethane and difluoromethane, and the observed rate constants for Q decay exhibit first-order dependence on substrate concentration (Fig. 2). The second-order rate constants for these reactions (Table 1) were obtained from the slopes of the respective k_{obs} versus [S] plots. At 20 °C and pH 7, KIE (k_H/k_D) values of 16 and 14.1 were obtained for fluoromethane and difluoromethane, respectively. The temperature dependence of Q decay was monitored for these substrates and linear Eyring plots were obtained (Fig. 3). The derived activation parameters are given in Table 1. The decay rate of Q is not affected by the presence of fluoroform (Fig. 2), indicating that no reaction occurs. This result agrees with previous kinetic studies, which report no degradation of fluoroform by sMMO under steady-state conditions [22].

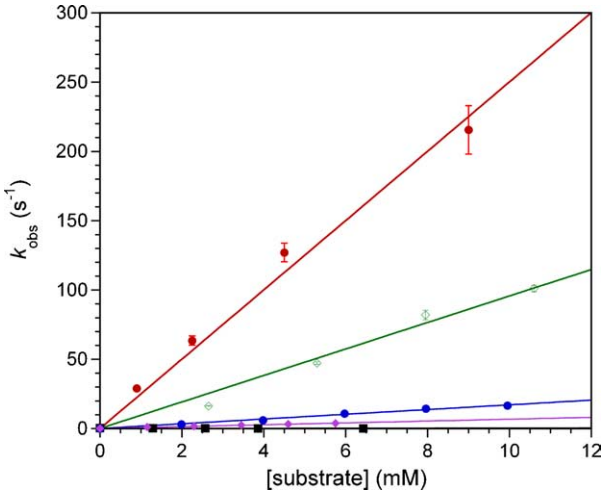

Fig. 2. Substrate concentration dependence of the kinetics of Q decay obtained from double-mixing experiments monitored at 420 nm with fluoromethane (red circles), fluoromethane-d_1 (blue circles), difluoromethane (green diamonds), difluoromethane-d_2 (purple diamonds), and fluoroform (black squares) at pH 7.0 and 20 °C.

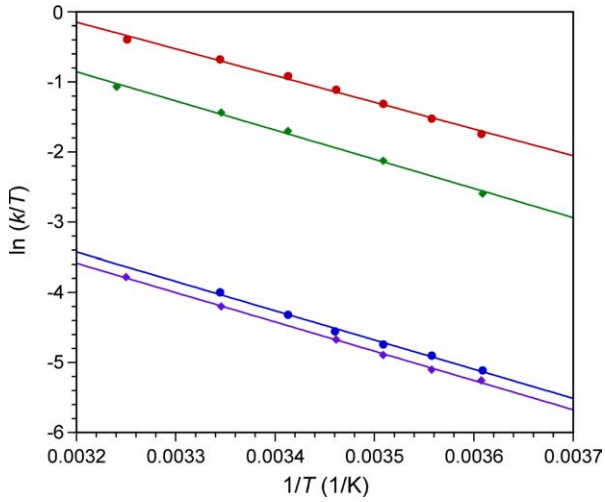

Fig. 3. Eyring plots for decay of the optical signal of Q after mixing with 4.5 mM fluoromethane (red circles), 2.1 mM fluoromethane-d_1 (blue circles), 5.3 mM difluoromethane (green diamonds), and 5.8 mM difluoromethane-d_2 (purple diamonds) at pH 7.0.

Discussion

Steady-state kinetic studies reveal that fluoromethane and difluoromethane, but not fluoroform, react with sMMO [22–24]. The putative product of fluoromethane oxidation is fluoromethanol, which is unstable and can undergo several decomposition reactions [25]. Double-mixing stopped-flow optical spectroscopic measurements yield a second-order rate constant for the reaction of Q with fluoromethane that is nearly identical to the one observed for methane (Table 1) [9]. Difluoromethane exhibits a smaller second-order rate constant for reaction with Q, and fluoroform does not react at all.

The QM/MM calculations predicted the KIE and activation free energy for reaction of Q with fluoromethane to be similar to those observed for nitromethane, but the present stopped-flow data reveal a large KIE indicative of tunneling at the transition state, and an Eyring analysis returns an activation free energy close to that of methane. The primary explanation for the computed large energy barrier was an unfavorable electrostatic interaction with a backbone carbonyl oxygen atom, which one would expect to be at least of the same magnitude in difluoromethane. Although difluoromethane does react more slowly than fluoromethane and methane, the activation enthalpy is only marginally closer to the 11.2 kcal/mol value observed for nitromethane [9], and the KIE is indicative of tunneling at the transition state. Taken together, these results indicate that fluoro- and difluoromethane are Class I substrates in their reactions with Q.

It is possible that the predicted electrostatic interaction between the fluorine and the carbonyl oxygen atoms does increase the free energy of activation but that this effect is partially offset by the lower homolytic bond dissociation energies for fluoromethane and difluoromethane (Table 1) compared to methane [26]. Apparently, the combination of electrostatic interactions and the much larger BDE of fluoroform are enough to prohibit reaction. Given the similar sizes of the three substrates to methane and their BDEs, this result is not surprising. For the other two fluorinated methanes, it would be possible in some rotameric conformers of the substrate to avoid the unfavorable electrostatic interaction with the Gly113 backbone carbonyl

Table 1
Rate constants and activation parameters for reactions of fluoromethanes with Q

Substrate	C–H BDE (kcal/mol)[a]	k (M^{-1} s^{-1})[b]	KIE (k_H/k_D)	$\Delta H^{\ddagger}$ (kcal/mol)	$\Delta S^{\ddagger}$ (cal/mol·K)[c]
CH_4[d]	104	28700 ± 900	23 ± 1	8.5 ± 0.3	−24 ± 1
CD_4[d]		1240 ± 50			
CFH_3	101	25000 ± 3000	16 ± 1	7.4 ± 0.4	−24 ± 1
CFD_3		1600 ± 100		8.27 ± 0.04	−27.5 ± 0.2
CF_2H_2	103	9300 ± 400	14.1 ± 0.5	9 ± 1	−20 ± 3
CF_2D_2		660 ± 50		8.5 ± 0.2	−27.0 ± 0.9
CF_3H	107	no rxn			

[a] Data taken from [26].
[b] Second-order rate constants determined from double-mixing stopped-flow experiments at pH 7.0 and 20 °C.
[c] Substrate concentrations for Eyring analysis: CFH_3 (4.5 mM), CFD_3 (2.1 mM), CF_2H_2 (5.3 mM), and CF_2D_2 (5.8 mM).
[d] Data taken from [9].

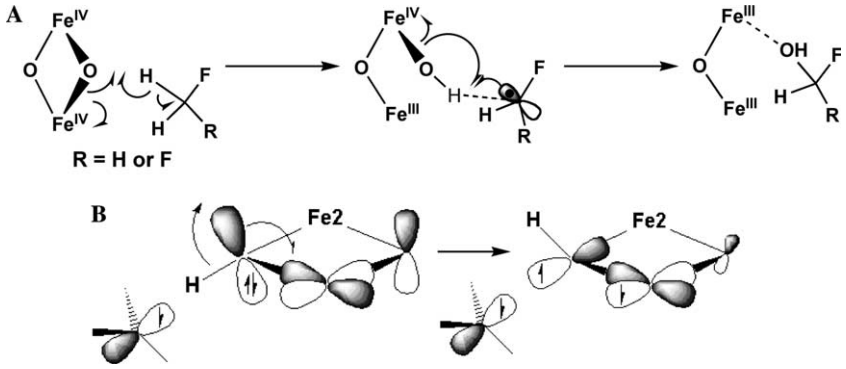

Fig. 4. (A) Proposed mechanism for the reaction of fluoromethanes with Q. In the first step, an electron is transferred to Fe2 with formation of a O–H bond and a bound fluoroalkyl radical. In the second step, the C–O bond forms with concomitant electron transfer to the second iron atom, Fe1. (B) Stereoelectronic details of the second electron transfer step depicting the metal-based LUMO of Fe1. If an α spin is transferred to Fe2 in the first step, the spin remaining on the bound alkyl radical is β. Since the iron atoms are coupled antiferromagnetically, the empty acceptor orbital on Fe1 has β character and will accept a β spin electron from the lone pair on the bridging oxygen atom. The α spin remaining on that oxygen p_π orbital will pair with the beta spin on the radical. Rotation of the O–H bond is essential for electron transfer to Fe1, positioning the oxygen p_π orbital for bond formation. A sub-picosecond lifetime of the fluoromethyl radical is anticipated for such a process.

oxygen atom. In these cases, the rate constant will also be influenced by the C–H BDEs, which correlate reasonably well with relative rates for similar substrates such as CF_nH_{4-n} ($n = 1$–3) in gas-phase H-atom abstraction reactions with the hydroxyl radical [27,28].

The KIEs observed for fluoromethane and difluoromethane are large and, like those observed for the reaction of Q with methane and acetonitrile [9], indicate that C–H activation is the rate-limiting step. Thus, a mechanism similar to that previously proposed for reactions of Q with methane is expected, in which substrate hydroxylation occurs via two sequential single electron transfer events (Fig. 4) [5,8]. The first electron transfer results in reduction of one Fe(IV) center, Fe2, to Fe(III) and formation of a bound fluoromethyl radical; it is the rate-determining step. Studies of MMO reactions with cyclopropane radical clock substrate probes and chiral ethane reveal a sub-picosecond radical lifetime, supporting this assignment [5]. Rotation of the H–O bond allows the β-electron of the oxo lone pair to transfer to the other Fe(IV) atom, Fe1, affording Fe(III) and positioning the oxygen atom for the formation of a C–O σ-bond (Fig. 4). Further details are provided in the figure caption.

This study was carried out to test a prediction of the QM/MM modeling of Q reactivity and to identify any areas in which the theoretical treatment might be inadequate. The results suggest that protein and substrate conformational changes accompanying hydrocarbon binding are quite important. Recent QM/MM calculations optimize the substrate fit with the active site pocket [29], and use of this technique for modeling the reactivity of Q may provide more accurate predictions. Moreover, the structure of H_{ox} was used as a starting model for the QM/MM optimizations. Since several protein residues distant from the active site differ between the reduced, diiron(II) and oxidized, diiron(III) structures [30,31], these residues should be optimized during the QM/MM calculations involving the structurally uncharacterized peroxo and Q intermediates. Finally, we note that the structure of the MMOH:MMOB complex is yet unknown. In the absence of MMOB, the hydroxylase is not an efficient catalyst. Although specific geometric differences that might occur between the H and H:B structures remain to be determined, a recent crystal structure analysis of product-bound H_{ox} protein revealed that a π-helix, composed of residues 202–211 in the four-helix bundle housing the catalytic diiron center, reorganizes upon bromohexanol binding such that residues 212–216, which were previously α-helical, are now part of the π-helix [32]. This conformational change increases the active site cavity volume, directs different residues toward the center of the bundle, and may possibly augur structural changes in MMOH induced by MMOB binding. Thus, further QM/MM studies should consider such possibilities.

In conclusion, although QM/MM calculations have done an excellent job modeling reactions of Q with most substrates, accuracy may be gained by probing additional protein and substrate conformations. Further reactions of the MMOH intermediates with a variety of substrates are currently in progress since they offer a valuable window on the chemical mechanisms of oxidative enzymes.

Acknowledgments

This work was supported by NIH Grant GM32134 from the National Institute of General Medical Sciences. L.G.B. was a Postdoctoral Trainee under NCI Cancer Training Grant CA09112. We thank Ms. Mi Hee Lim and Ms. Elizabeth Nolan for experimental assistance, and Prof. Richard Friesner for helpful discussions.

References

[1] P.E.M. Siegbahn, Mechanisms of metalloenzymes studied by quantum chemical methods, Q. Rev. Biophys. 36 (2003) 91–145.
[2] R.J. Deeth, Computational bioinorganic chemistry, Struct. Bond. 113 (2004) 37–69.

[3] A. Ghosh, P.R. Taylor, High-level ab initio calculations on the energetics of low-lying spin states of biologically relevant transition metal complexes: a first progress report, Curr. Opin. Chem. Biol. 7 (2003) 113–124.
[4] M. Merkx, D.A. Kopp, M.H. Sazinsky, J.L. Blazyk, J. Müller, S.J. Lippard, Dioxygen activation and methane hydroxylation by soluble methane monooxygenase: a tale of two irons and three proteins, Angew Chem. Int. Ed. 40 (2001) 2782–2807, and references cited therein.
[5] M.-H. Baik, M. Newcomb, R.A. Friesner, S.J. Lippard, Mechanistic studies on the hydroxylation of methane by methane monooxygenase, Chem. Rev. 103 (2003) 2385–2419, and references cited therein.
[6] B.F. Gherman, M.-H. Baik, S.J. Lippard, R.A. Friesner, Dioxygen activation in methane monooxygenase: a theoretical study, J. Am. Chem. Soc. 126 (2004) 2978–2990.
[7] P.E.M. Siegbahn, A comparison of dioxygen bond-cleavage in ribonucleotide reductase (RNR) and methane monooxygenase (MMO), Chem. Phys. Lett. 351 (2002) 311–318.
[8] B.F. Gherman, S.J. Lippard, R.A. Friesner, Substrate hydroxylation in methane monooxygenase: quantitative modeling via mixed quantum mechanics/molecular mechanics techniques, J. Am. Chem. Soc. 127 (2005) 1025–1037.
[9] E.A. Ambundo, R.A. Friesner, S.J. Lippard, Reactions of methane monooxygenase intermediate Q with derivatized methanes, J. Am. Chem. Soc. 124 (2002) 8770–8771.
[10] B.J. Wallar, J.D. Lipscomb, Dioxygen activation by enzymes containing binuclear non-heme iron clusters, Chem. Rev. 96 (1996) 2625–2657.
[11] A.M. Valentine, S.S. Stahl, S.J. Lippard, Mechanistic studies of the reaction of reduced methane monooxygenase hydroxylase with dioxygen and substrates, J. Am. Chem. Soc. 121 (1999) 3876–3887.
[12] L.G. Beauvais, S.J. Lippard, Reactions of the peroxo intermediate of soluble methane monooxygenase hydroxylase with ethers, J. Am. Chem. Soc. 127 (2005) 7370–7378.
[13] B.J. Brazeau, J.D. Lipscomb, Kinetics and activation thermodynamics of methane monooxygenase compound Q formation and reaction with substrates, Biochemistry 39 (2000) 13503–13515, and references cited therein.
[14] S.J. Lippard, Hydroxylation of C–H bonds at carboxylate-bridged diiron centers, Phil. Trans. R. Soc. A 363 (2005) 861–877.
[15] B.J. Brazeau, J.D. Lipscomb, Thermodynamic and kinetic evidence for a two-step reaction between methane monooxygenase compound Q and substrates, Intern. Congr. Ser. 1233 (2002) 229–233.
[16] G.T. Gassner, S.J. Lippard, Component interactions in the soluble methane monooxygenase system from *Methylococcus capsulatus* (Bath), Biochemistry 38 (1999) 12768–12785.
[17] D.E. Coufal, J.L. Blazyk, D.A. Whittington, W.W. Wu, A.C. Rosenzweig, S.J. Lippard, Sequencing and analysis of the *Methylococcus capsulatus* (Bath) soluble methane monooxygenase genes, Eur. J. Biochem. 267 (2000) 2174–2185.
[18] D.A. Kopp, G.T. Gassner, J.L. Blazyk, S.J. Lippard, Electron-transfer reactions of the reductase component of soluble methane monooxygenase from *Methylococcus capsulatus* (Bath), Biochemistry 40 (2001) 14932–14941.
[19] E. Wilhelm, R. Battino, R.J. Wilcock, Low-pressure solubility of gases in liquid water, Chem. Rev. 77 (1977) 219–262.
[20] M. Albert, W. Repetschnigg, J. Ortner, J. Gomes, B.J. Paul, C. Illaszewicz, H. Weber, W. Steiner, K. Dax, Simultaneous detection of different glycosidase activities by ^{19}F NMR spectroscopy, Carbohydr. Res. 326 (2000) 395–400.
[21] F.J. Weigert, Fluorine magnetic resonance spectra of monofluoro- and difluoro-substituted hydrocarbons, J. Org. Chem. 45 (1980) 3476–3483.
[22] G.M. King, Stability of trifluoromethane in forest soils and methanotrophic cultures, FEMS Microbiol. Ecol. 22 (1997) 103–109.
[23] L.J. Matheson, L.L. Jahnke, R.S. Oremland, Inhibition of methane oxidation by *Methylococcus capsulatus* with hydrochlorofluorocarbons and fluorinated methanes, Appl. Environ. Microbiol. 63 (1997) 2952–2956.
[24] L.G. Miller, C. Sasson, R.S. Oremland, Difluoromethane, a new and improved inhibitor of methanotrophy, Appl. Environ. Microbiol. 64 (1998) 4357–4362.
[25] H. Hou, J.-Z. Guo, C.-P. Liu, Y.-S. Gu, Theoretical investigation of the decomposition of monofluoromethanol, Chin. J. Chem. 16 (1998) 213–218.
[26] Y.-R. Luo, Handbook of Bond Dissociation Energies in Organic Compounds, CRC Press, Boca Raton, 2002.
[27] K.-M. Jeong, F. Kaufman, Kinetics of the reaction of hydroxyl radical with methane and with nine Cl- and F-substituted methanes. 1. Experimental results, comparisons, and applications, J. Phys. Chem. 86 (1982) 1808–1815.
[28] K.-M. Jeong, F. Kaufman, Kinetics of the reaction of hydroxyl radical with methane and with nine Cl- and F-substituted methanes. 2. Calculation of rate parameters as a test of transition-state theory, J. Phys. Chem. 86 (1982) 1816–1821.
[29] A.E. Cho, V. Guallar, B.J. Berne, R. Friesner, Importance of accurate charges in molecular docking: quantum mechanical/molecular mechanical (QM/MM) approach, J. Comput. Chem. 26 (2005) 915–931.
[30] D.A. Whittington, S.J. Lippard, Crystal structures of the soluble methane monooxygenase hydroxylase from *Methylococcus capsulatus* (Bath) demonstrating geometrical variability at the dinuclear iron active site, J. Am. Chem. Soc. 123 (2001) 827–838.
[31] M.H. Sazinsky, J. Bard, A. Di Donato, S.J. Lippard, Crystal structure of the toluene/*o*-xylene monooxygenase hydroxylase from *Pseudomonas stutzeri* OX1, J. Biol. Chem. 279 (2004) 30600–30610.
[32] M.H. Sazinsky, S.J. Lippard, Product bound structures of the soluble methane monooxygenase hydroxylase from *Methylococcus capsulatus* (Bath): protein motion in the α-subunit, J. Am. Chem. Soc. 127 (2005) 5814–5825.